International Journal of Hybrid Information Technology
Vol.7, No.5 (2014), pp.323-340
http://dx.doi.org/10.14257/ijhit.2014.7.5.30

Crack Analysis of Multi-plate Intersection Welded Structure in Port Machinery Using Finite Element Stress Calculation and Acoustic Emission Testing

Lu Kai-liang, Zhang Wei-guo, Zhang Ye, Huang Hui, Chen Yi-sheng, Li Wen-yuan and Wang Chao

Logistics Engineering College, Shanghai Maritime University
lkl1984@163.com

Abstract

Crack is the main inducement of failure accidents in welded structures of port machinery. Taking actual engineering problems occurred in a coal wharf as a case where a stacker reclaimer altered its local structure (bucket wheel changed to be chute) and then cracks appeared on the Slew deck with pylon after half a year. Using the finite element simulation combined with acoustic emission testing, the stress concentration and crack active status of the multi-plate intersection welded structure were inspected, which aimed at monitoring the development trend of the cracks and finding out reasons. Finite element stress calculation method adopts Solidworks, ANSYS and Hypermesh software co-simulation to explore the effects of mesh type and density on the stress calculation results of the Slew deck with pylon structure, and to analyze the stress distribution of the multi-plate intersection shell structures. According to the analysis results, this paper infers the reasons for crack propagation. Combined with the regular monitoring of acoustic emission testing technology on the active state of cracks and the intensity of expansion, the influences on the apparatus are deduced by the crack states of the bucket wheel reclaimer operations under different working conditions. And then put forward measures for a whole reasonable structure of the rectification and crack repair plans. The results of the research show that: 1) The maximum stress value following the change decreases slightly，which indicates that structure change is not the direct reason for cracking, instead, it is the initial structure design problems; 2) The imbalance torque produced in the boom hinge point after the change is the direct reason for causing cracks; 3) The proposed repairing scheme significantly reduces the stress at the cracks, and improves the fatigue strength. Finite element simulation combined with acoustic emission testing method provides effective means for analysis and prediction of cracks occurred in multi-plate intersection welded structure of port machinery.

Keywords: *Port, Multi-plate intersection welded structure, Crack analysis, Load allocation, Finite element simulation, Acoustic emission testing*

1. Introduction

Steel structures are normally connected by welding without exception for that of the port machinery equipment. Compared with the former steel structures fixed by rivets or bolts in early stage, the welded steel structure is more vulnerable under fatigue states and likely to causing greater hazards by welding cracks which are the major cause for the malicious events of the welded forms.

Many approaches have been adopted to analyze fatigue mechanism of the weld joint, and

ISSN: 1738-9968 IJHIT

those methods are classified by the parameters depicting the fatigue life or fatigue strength [1], in general, the processes can be summarized as follows: (1)Nominal stress approach, depends on the properties of related cross sections, internal as well as external loads to determine the range of itself; (2) Structural or hot-spot stress approach, takes the range of structural stress and the discontinuity of the structures into consideration at the same time; (3) Notch stress and notch intensity approach, applies the range of the elastic notch stress or the equivalent parameters, such as the influence to the notch caused by the stress intensity, as the objects to consider; (4) Notch strain approach, describes related damage process in the material by the range of local elastic-plastic strain; (5) Crack propagation approach, using particular parameters, such as J-integral or the range of stress intensity, depicts cycle growth of the crack length, *i.e.*, the crack propagation rate.

Regarding to the nominal stress approach, standard S-N curves [2, 3] were adopted together with detail classes of basic joints to analyze it initially. Later, new methods, naming a hboomonized set of S-N curves and an associated catalogue of details, were accepted internationally. But Petinov *et al.*, [4] pointed it out that this approach detached similitude between test specimen and the real structures, besides it failed to consider the influence of the surrounding structures and loads, resulting in apparent disparity with the theory values especially when dealing with local analysis.

Excluding the local analysis process, structural or hot-spot stress approach directly focuses on increase of components stress for the whole structural configuration by the macro-geometry thought. This technique depends on the plate or shell thickness for that it requires several reference points at certain distances away from the weld for analysis via stress and extrapolation. This way can assess and evaluate more precisely overall situation of stress for components and fatigue, nevertheless, there are no explicit rules for the selection of the reference points, as well, it have no regard for the flat notch which cannot be taken as parameter[5], i.e. the welding edge, leading to lower precision of results.

Notch stress and notch intensity approach, emphasizing on microstructure support hypothesis, designs a fictitious radius r_f so as to directly analyze local stress without additional consideration of fatigue notch factor or stress concentration factor, and this approach is based on elastic theory and numerical methods, such as finite element, boundary element method. In addition, it considers the various geometric [6-9] factors for higher accuracy. However, when considered different loading phase or half plastic metal (such as aluminum alloy), the component fatigue prediction efficiency conducted by this method significantly reduced.

As for notch strain approach, it focuses on elastic stress and strain analysis of slit, and considers the local stress strain effect on the surrounding material and recycle material behavior, gaining the best effects for stress analysis of base material incision. For example, through stress strain relationship and the determination of the crack initiation life value can fully illustrate the feasibility of this method [10].

Another frequently-used method, namely crack propagation approach based on the analysis for welded joint fatigue assessment, measures the initial crack length. Making it particularly suitable to assess structural members with flaws or other crack-like defects, and it has been applied to special geometric factor analysis of the influence of the fatigue life, for example, the technique can be helpful to research longitudinal attachments [11] and cross joint dislocation [12] as well as the influence of residual stress. On the whole crack propagation method focuses on two aspects, on the one hand it concentrates on crack ratio and the influence of the transmission, McClung proposed finite element method (FEM) [13] to execute crack closure model problems and describe the application of finite element method. On the other hand, it refers to incision strain method and crack behavior relating to crack

closure. Newman *et al.*, [14] put it forward that It has introduced the plastic loop area and correction for the range of constraint coefficient; Hou and Charng [15] found that FEM analysis based on the short crack propagation generates more consistent results than those conducted by local analysis method. These two aspects is of great significance to the serious accidents of the machinery for steel structure and expanding the utility of aging structure. Therefore, FEM plays the key role in evaluating residual life, structural redundancy and establishing a reasonable inspection plan.

A certain coal terminal put a stacker reclaimer, with the stacking capacity of 3840t/h and reclaiming capacity of 6000t/h, into use in 2003. Then a structural change occurred in 2010, the stacker reclaimer is just used for stacking. Figure 1 shows that bucket wheel mechanism has been removed from the head of stacker reclaimer while adding a chute weighing 6.5t. In total, actual lost weight of head is 27.9t, and 53.08t decrease in counter weight.

Figure 1. Change of the Stacker Reclaimer Structure (bucket wheel changed to be chute)

After structural change, the machine owns a stacking capacity of 1000t/h in terms of the lump coal within the diametre of 80mm, and is able to stack spray coal directly under special cases with the capacity of 2000t/h. Cracks appeared after the equipment ran for just more than half a year through the structural change. They are loacted at the place where boom support connects with slew deck, as shown in Figure 2.

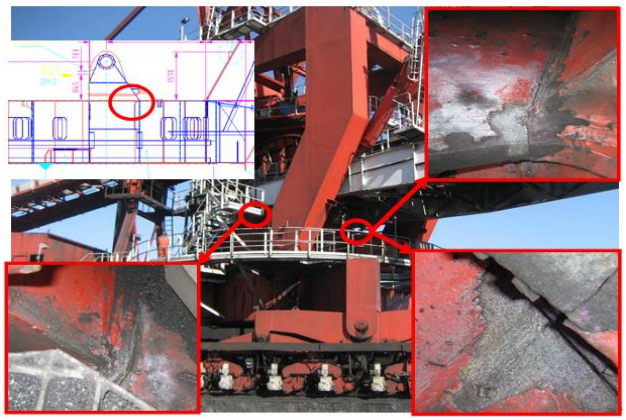

Figure 2. Schematic Diagram of the Cracks' Location in the Slew Deck with Pylon

This paper introduces a method that adopts FEM, combined with Solidworks, ANSYS and

Hypermesh for joint simulation as well as acoustic emission (AE) testing, to analyze and inspect the structure stress concentration and crack states, aiming at monitoring crack development trend, also in search of causes for structure cracks, and generates structure rectification measures and crack repair scheme.

2. Structure Rectification and Reaction Force Calculation

Solidworks model for structure of Slew deck with pylon is shown in Figure 3. Judged by experience, the main cause of the cracks is the loads on cantilever beam and counterweight beam, which often manifests itself in cantilever beam hinge point or counterweight beam hinge point, resulting in unbalance torque.

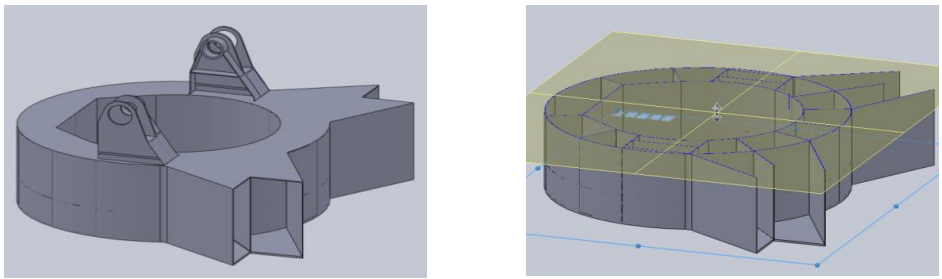

(a) Multi-plate Intersection Entire Model (b) Section View of Multi-Plate Intersection

Figure 3. Slew Deck with Pylon Structure Solidworks Model

Via conducting the analysis of the tail weight adjustment to the stacker reclaimer, it indicates the issue of boom hinge point where an unbalanced movement equaling to 3.153×10^{5} t□mm exists after the change. In order to eliminate such unbalance, it is recommended that increasing weight of 5.74t at the bucket-wheel without changing the tail weight. Finite element analysis should be applied for the sake of further definition of the cracking reasons for the Slew deck with pylon.

The prerequisite is to specify the force loading and constraint conditions on Slew deck with pylon so as to conduct finite element simulation calculation. Assuming that Slew deck with pylon respect to the upper structure (including the bucket, bucket wheel boom, belt transmission system, balance beam) is in the resting state, so load on the Slew deck with pylon is mainly the applied force focused on the luffing cylinder hinge point and balance beam hinge point on upon structure.

There is few force on the structure in the direction of *Z*, according to the relationship of connection structure components, schematic diagram of calculation of plane frame structure for bucket wheel stacker reclaimer superstructure (boom luffing angle of 15) is shown in Figure 4.

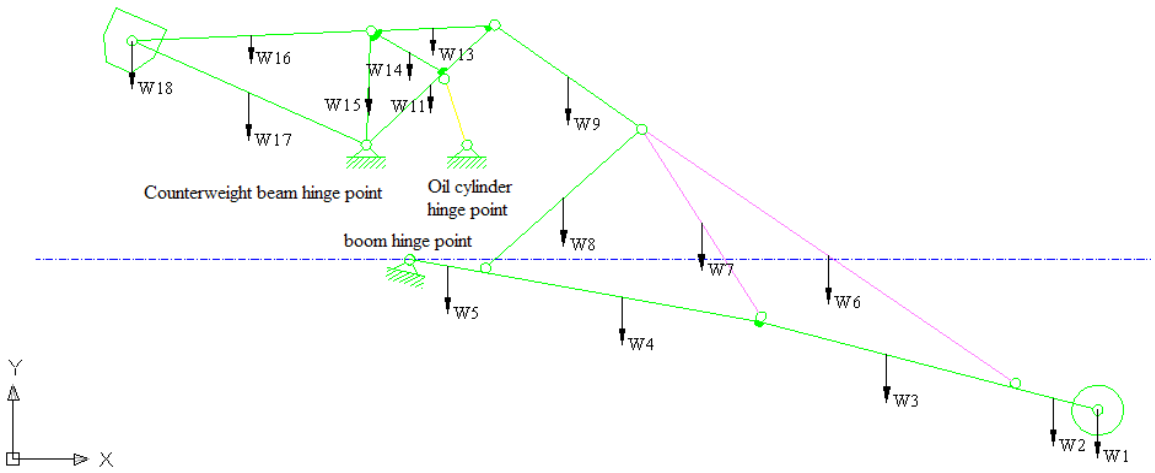

Figure 4. Bucket Wheel Reclaimer Structure Calculation Diagram

The hinge point forces of jib in different luffing angles are listed in Table 1.

Table 1. Hinge Point Forces (Unit: kN)

Phase	Hinge point location	Code name	The boom luffing angles					
			-8 °		0 °		+15 °	
Before the change	Boom hinge point	Fx_a1	2173		2170		2113	
		Fy_a1	808		595		292	
	Oil cylinder hinge point	Fx_b1	1915		1382		523	
		Fy_b1	-2607		-2407		-1648	
	Counterweight beam hinge point	Fx_c1	-4088		-3552		-2636	
		Fy_c1	7012		7025		6569	
After the change	Boom hinge point	Fx_a2	1884		1884		1840	
		Fy_a2	816		630		363	
	Oil cylinder hinge point	Fx_b2	1449	Resultant force (pull) **2448**	1023	Resultant force (pull) **2056**	358	Resultant force (pull) **1182**
		Fy_b2	-1973		-1783		-1126	
	Counterweight beam hinge point	Fx_c2	-3333		-2907		-2198	
		Fy_c2	5722		5718		5328	
After rectification	Boom hinge point	Fx_a2	2019		2018		1969	
		Fy_a2	809		611		327	
	Oil cylinder hinge point	Fx_b2	1273		881		281	
		Fy_b2	-1733		-1525		-884	
	Counterweight beam hinge point	Fx_c2	-3292		-2899		-2250	
		Fy_c2	5447		5437		5080	

Table 1 shows that:

(1) Joint force of hinge points in each luffing angle after structure changes is generally less than that before the change, and only the boom hinged vertical (*y* direction) force increases; because the weight of the upper structure counts less than those before the change. The cylinder and the balance beam hinge point force after the rectification is generally less than that after the change. Only the boom hinge point (*x* direction) increases lateral force because

of the elimination of the unbalanced moment after the rectification, but the boom end of bucket wheel increases weight of 5.74t.

(2) The table lists the cylinder after the change (1 on each side, 2 in total) tensile force size, -8°, 0°, 15° respond to respectively 249.8t,209.8t,120.6t, and the hydraulic test results of cylinder in the tendency and value are identical, indicating that the calculation of hinge point force value is reliable. The numerical simulation results error is partially due to: 1) the center of gravity position deviation of each member; 2) friction of the hinge point is not considered in the simulation, *etc.*

3. Finite Element Stress Calculation

3.1 Slew Deck with Pylon Structure Finite Element Model

SHELL63 and SOLID45 elements were combined to model the Slew deck with pylon by ANSYS software. The ladder, aisle and additional weight loading distribution on the Slew deck with pylon were added to the corresponding nodes as concentrated mass. Total mass of the model is 106782kg. Fixed constraints were applied to the nodes of bolts in the slew deck bottom plate. The force of the whole structure in horizontal direction where it is perpendicular to the boom is small, so the main consideration of the force is located at vertical and the direction along the boom horizontally. Concentrated loads were applied to the hinge point, and in order to avoid stress concentration, rigid regions were set in the hinge point. Structure finite element model is shown in Figure 5, a total of 24551 SHELL63 elements, 7776855 SOLID45 elements.

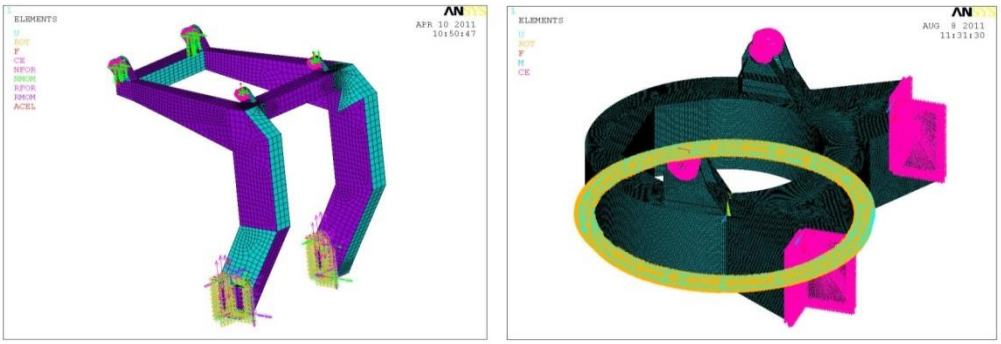

(a) SHELL63 Part (b) SOLID45 Part

Figure 5. Slew Deck with Pylon FEM Model

3.2 Meshing Impact on the Simulation Results

Generally speaking, meshing (including the mesh density, mesh type *etc.*,) can impose great effects on stress calculation results of finite element structure, especially on stress concentration, Example results in Figure 6 show that: when the grid size is 0.03, stress distributions calculated by tetrahedral and hexahedral mesh are similar, but the maximum stress value in concentrated force acting position exhibits larger deviation (944MPa and 1340MPa respectively); while the grid size is reduced to 0.02, the stress distribution of tetrahedral and hexahedral mesh is consistent with each other, the maximum stress concentration seems very close to the value (1000MPa and997MPa). Therefore, in this case, when the mesh density is 0.02, the mesh type is supposed to exert no effects on the simulation results.

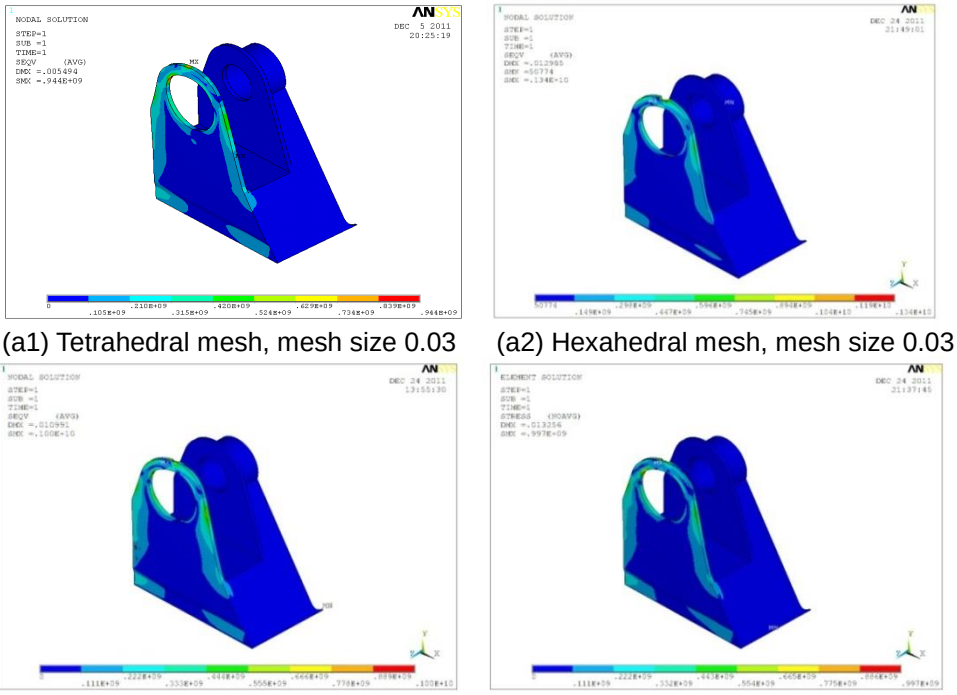

(a1) Tetrahedral mesh, mesh size 0.03 (a2) Hexahedral mesh, mesh size 0.03

(b1) Tetrahedral mesh, mesh size 0.02 (b2) Hexahedral mesh, mesh size 0.03

Figure 6. Influence of Mesh Type, Mesh Density on Finite Element Stress Calculation Results

The solid model established by Solidworks was then imported to Hypermesh and used tetrahedral mesh with mesh size of 0.02, then imported into ANSYS for calculation.

3.3 Finite Element Simulation Results

The maximal stress values at the crack position before and after the change are exhibited in Table 2.

Table 2. Stress Results under Different Boom Luffing Angles

Luffing angle	Stress value before the change (MPa)		Stress value before the change (MPa)	
	Left	Right	Left	Right
-8 °	182	130	156	111
0 °	187	133	161	114
+15 °	190	136	163	117

When the boom luffing angle is 15, the Von Mises stress distribution on Slew deck with pylon structure is shown in Figure 7.

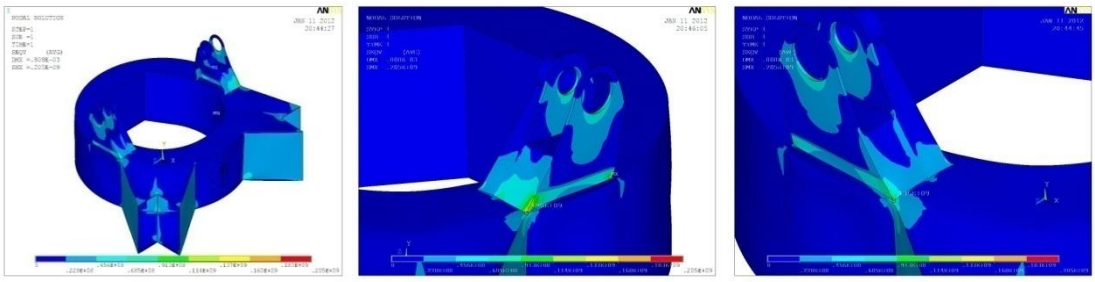

1) The Overall Stress 2) Left 3) Right

(a) The Boom Luffing Angle of 15°, Before the Change

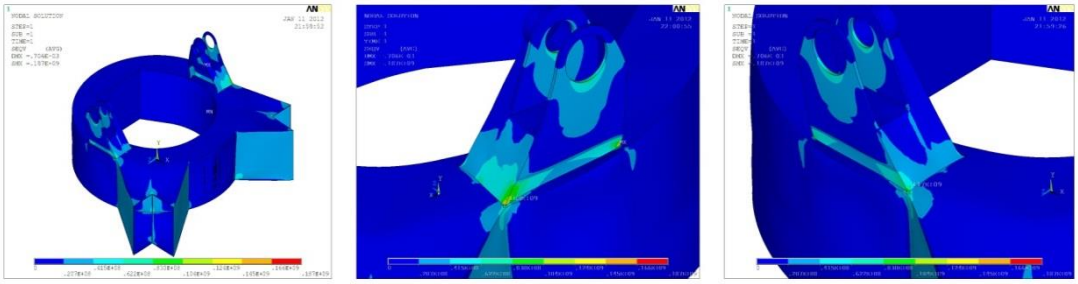

1) The Overall Stress 2) Left 3) Right

(b) The Boom Luffing Angle of 15°, After the Change

Figure 7. Von Mises Stress Distribution of Slew Deck with Pylon Structure

From Table 2, we can know, maximal stress values under different luffing angle after the structure change are smaller than that before the change, which is consistent with the reaction force change trends of the hinge points shown in Table 1. The stress values on the left side are generally about 40-50 MPa larger than that on the right side. Compared in Figure 7, the stress distribution of the Slew deck seems little change before or after the structure change, and there is a decreasing trend after the change.

4. Acoustic Emission Testing

4.1 Test Principle

Acoustic emission (AE) is a phenomenon where local material for energy rapidly releases and generates transient elastic wave; acoustic emission testing technology is the application of material acoustic emission phenomenon, with nondestructive testing technology to infer the dynamic activity of material defects. The detection principle is shown in Figure 8. Compared with other non-destructive detection technology, acoustic emission detection has the characteristics of dynamic, real-time, complete, continuous, but defect analysis in the actual detection practice basically still stays on the qualitative analysis. Such technology has become an important means for large and complex component for online survey and monitoring due to the four essential characteristics of acoustic emission testing technology, and it is widely used in aerospace, shipbuilding, chemical, petrochemical, nuclear industry, bridge, port engineering, *etc*.

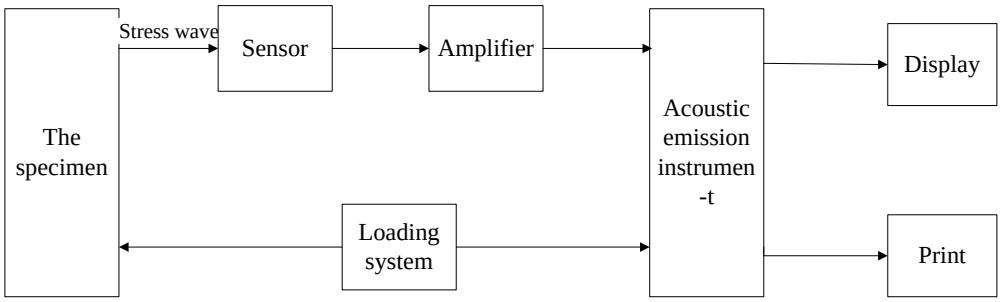

Figure 8. Diagram of Acoustic Emission Testing Principle

The crack location on Slew deck with pylon of the stacker underwent 6 acoustic emission tests on June 16th, August 12th, September 15th, October 27th, December 15th in 2011 and January 4th, 2012. Due to limitations of site conditions, of which only the first 3 times focused on the upper wing plate and web cracks of the Slew deck with pylon for the acoustic emission test (sensor arrangement scheme No.1), and the other tests were executed on the left wing, left web and right wing crack positions (sensor arrangement scheme No.2).

4.2 Test Equipment

The test equipment is SAMOS 8 channels digital acoustic emission system produced by PAC Company in United States (shown as Figure 9). The system can realize simultaneously real-time collection, storage and display for waveforms as well as acoustic emission characteristic parameters for all the eight channels. Accessories include sensor, preamplifier, computer and cables *etc*. Select R15 type 150 kHz resonance frequency high sensitivity sensor, and adopt the 2/4/6 type one produced by PAC Company, which has the merits of multiple gain, high signal-to-noise ratio and other characteristics. The preamplifier dynamic range is more than 82 dB.

(a) System composition (b) System on field testing

Figure 9. 8 Channels Acoustic Emission Detection System

4.3 Sensor Arrangement

Two kinds of sensor layout were utilized. In scheme No. 1, sensors were arranged only for Slew deck with pylon on the left wing plate and the left external web crack location, while no sensors on the right side of cracks, which are shown in Figure 10.

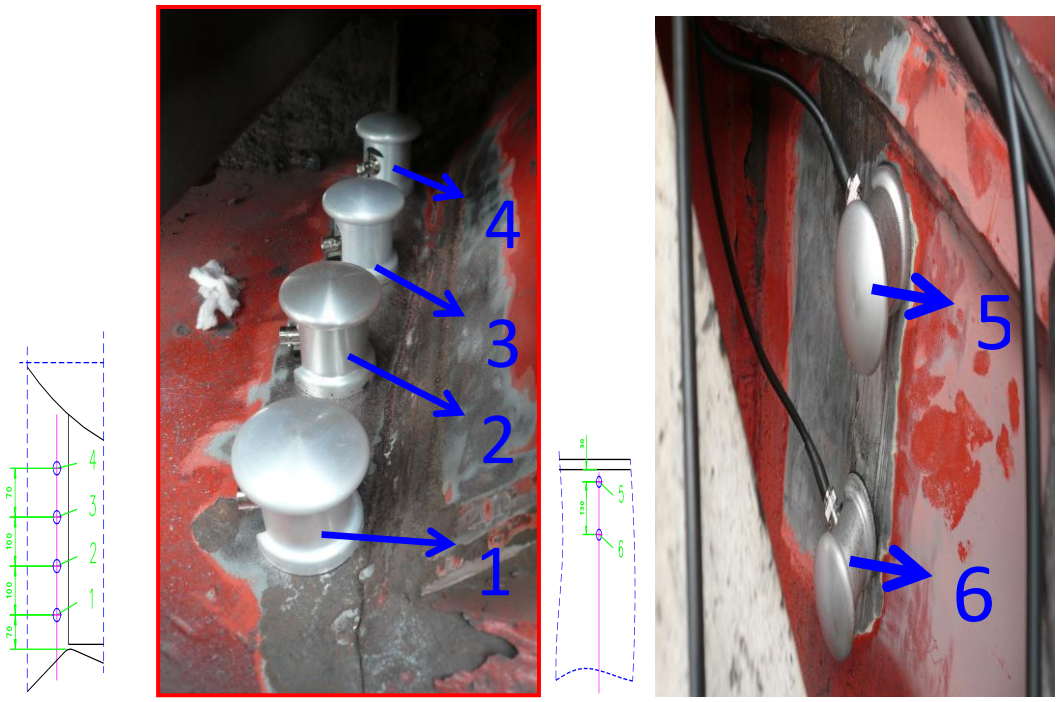

(a)Layout on the Left Wing Plate (b) Layout on the Left External Web

Figure 10. Sensor Arrangement Scheme No.1 for the Slew Deck with Pylon Cracks

In scheme No.2, sensors were arranged on the left wing plate, left external web cracks and right wing plate of the Slew deck with pylon (shown as Figure 11). The first 3 AE tests chose the sensor arrangement scheme No.1, and the following 3 acoustic emission tests adopted arrangement scheme No.2.

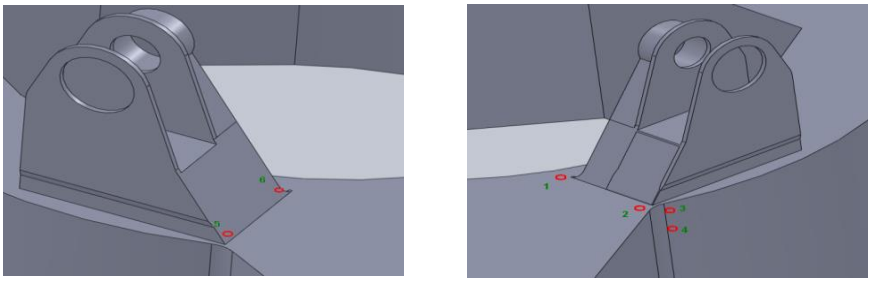

(a) Layout on the right wing plate (b) Layout on the left wing plate, left external web

Figure 11. Sensor Arrangement Scheme No.2 for the Slew Deck with Pylon Cracks

4.4 Test Parameters and Working Conditions Setting

The field test shows that, the acoustic emission signal frequency of the structure ranges from 50-350 kHz. According to the noise level, the threshold value is set as 45 dB; analog filter with lower limit of 20 kHz and ceiling of 400 kHz

Due to the site and scheduling constraints, six working conditions were chosen to do acoustic emission tests, as listed in Table 3.

Table 3. Test Working Conditions Setting

Conditions No.	Condition descriptions	1st test	2nd test	3rd test	4th test	5th test	6th test
1	No loads on the belt; gantry and the main boom support is fixed	-	-	-	-	Y	Y
2	No loads for gantry travelling; the main boom is parallel to the conveyor belt	-	Y	Y	Y	-	-
3	No loads; the main boom luffing operation	-	Y	Y	Y	-	Y
4	No loads; the main boom rotary operation	-	Y	Y	Y	-	Y
5	Loading; the main boom luffing operation	Y	Y	Y	Y	-	Y
6	Loading; the main boom rotary operation	Y	Y	Y	Y	-	-
7	Loading; gantry and the main boom support is fixed	Y	Y	Y	Y	Y	Y

4.5 Test Results Analysis and Discussion

4.5.1 Analysis of crack status site check

Both sides of the Slew deck with pylon crack position are basically the same, the crack propagation on the left side of is shown in Figure 12. Left wing crack length on the Slew deck with pylon is about 27 cm, accounting for 30% size of the upper wing plate along the direction, and the length of the outer web plate crack is about 5.5 cm. Internal inspection into the slew deck shows, crack positions on the left wing plate and outer web plate are sheltered by the clapboard, which makes it impossible to measure the position of weld length within the left wing plate. Plate located in the left wing plate cracks intersection weld has cracked thoroughly, so there are a large amount of dust into the chamber.

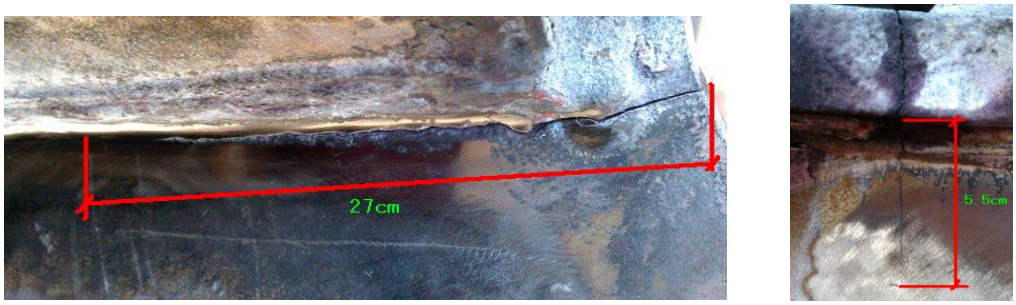

(a) Crack Length on the Left Wing (b) Crack Length on the Outer Web Plate

Figure 12. Crack Propagation on the Left Side of the Slew Deck with Pylon

4.5.2 Analysis and discussion of the acoustic emission testing results

In order to facilitate the comparison, different conditions on Slew deck with pylon cracks by acoustic emission characteristics are analyzed under the same sampling time of 200 seconds.

(1) No loads on the belt; gantry and the main boom support is fixed (Condition 1)

Figure 13 shows the comparison between the fifth and the sixth tests, which demonstrates under the same conditions, there are some differences between the two results.

Namely, in the fifth test under Condition 1 both sides of the Slew deck with pylon cracks generated a certain number of acoustic emission source signals, showing that this condition will have certain influence on the crack extension. While in the sixth test, the test results indicate Condition 1 does not affect either the left or right side of crack propagation. The

main reason for the difference is speculated that stacker reclaimer was located at different pile position during the two tests, and the relative height difference of the crane rail wheels might affect the stress condition at the Slew deck with pylon cracks, which leads to different acoustic emission testing results. But attention should be paid to that under Condition 1 damage has been caused to the Slew deck with pylon cracks, indicating that the cracks or bearing welds are active.

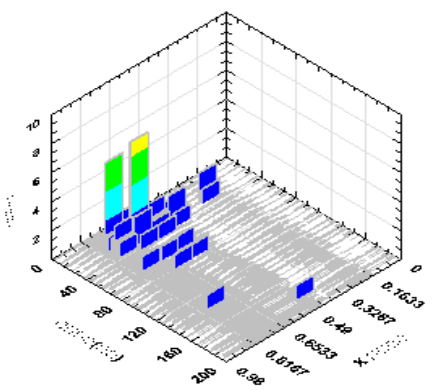

(a1) The Left Wing, 5th test

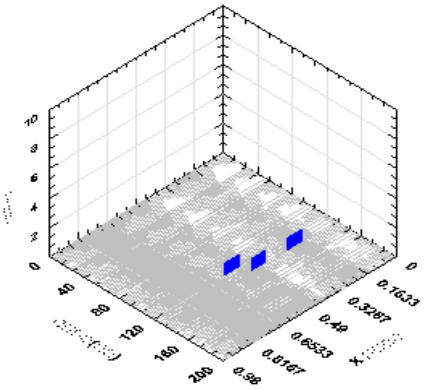

(a2) The Left Wing, 6th Test

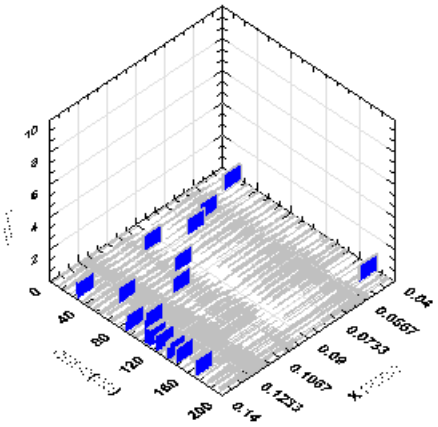

(b1) External Left Web, 5th Test

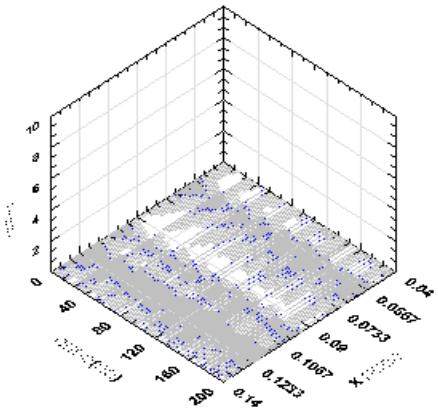

(b2) External Left Webs, 6th Test

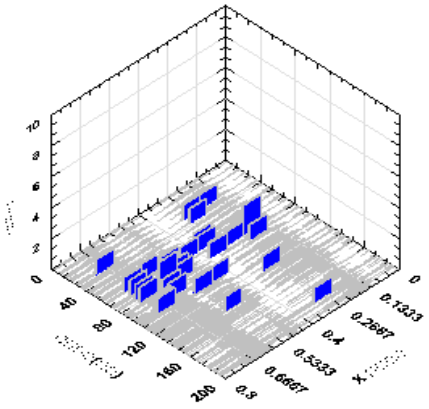

(c1) the right wing, 5th test

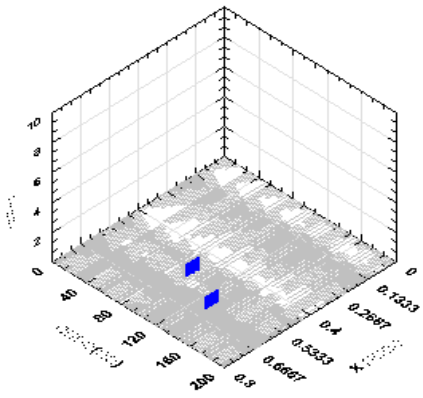

(c2) the right wing, 6th test

Figure 13. Acoustic Emission Location Map under Condition 1

(2) No loads for gantry travelling; the main boom is parallel to the conveyor belt (Condition 2)

The second and the third test results are compared. Through AE location map, a number of acoustic emission source signals were produced on the left wing plate cracks of the Slew deck with pylon, but the left external web crack position found no signals. It is known that there are some adverse effects on the extension of left wing cracks under Condition 2, and have few effects on the left outer web cracks of the Slew deck with pylon.

(3) No loads; the main boom luffing operation (Condition 3)

Taking the second, the third, and the forth test comparison analyses as an example, Condition 3 have some adverse effects on both sides of wing cracks propagation, and basically no influences on the left side web crack propagation.

(4) No loads; the main boom rotary operation (Condition 4)

Comparing the second, the third, the fourth and the sixth test results, Condition 4 have certain effects on the cracks expansion on the both sides of wing cracks, instead, exerts no influences on the external web cracks propagation.

(5) Loading; the main boom luffing operation (Condition 5)

Comparing the second, the third, the fourth, and the sixth test results, Condition 5 imposes more affection on both sides of the wing plate around the crack extension, and bearing welds displayed signs of cracking, which deserves close attention to avoid multiple crack coalescence phenomenon. But no AE source signals occurred on the left external web position basically, showing that crack extension of outer web receives few effects.

(6) Loading; the main boom rotary operation (Condition 6)

Comparing the second, the third, the fourth test results, Condition 6's effects on the cracks are almost the same as Condition 5's.

(7) Loading; gantry and the main boom support is fixed (Condition 7)

The first, the third, the fourth, and the sixth test results are compared, as shown in Figure 14. The results depicts that Condition 7 generates a number of AE location source signals on both sides of wing cracks, especially in the sixth test, the left and right cracks on the wing plate and the left external web cracks are quite active, and a large number of acoustic source signals are found at the bearing welds paralleled to the direction of the cracks, which shows the tendency of crack propagation has become more active, and the bearing welds exhibit cracking signs. At the same time, it is found that in sixth tests, the left outer web cracks also contains a number of acoustic emission source signals, indicating the cracks at this position are also in active state.

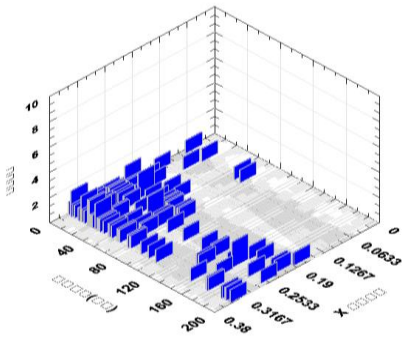

(a1) The Right Wing, 1st Test

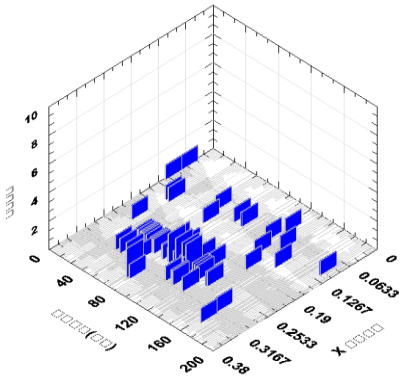

(a2) The Right Wing, 3rd Test

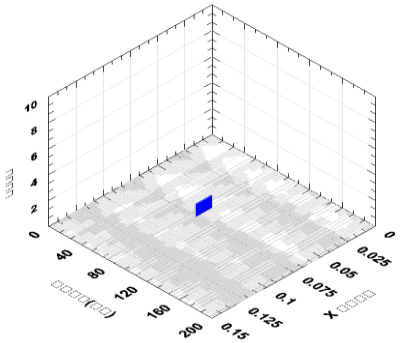

(b1) External Left Web, 1st Test

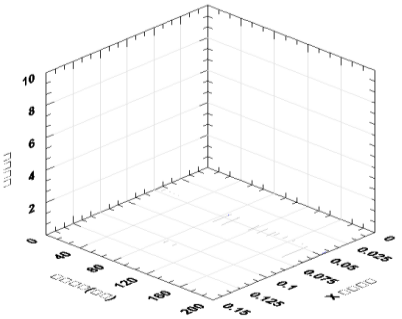

(b2) External Left Web, 3rd Test

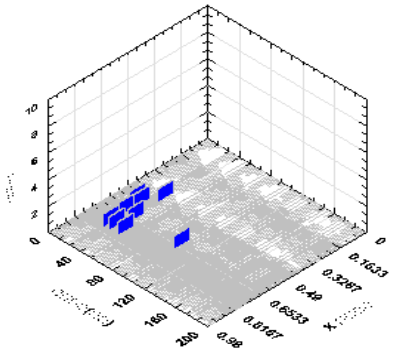

(c1) The Left Wing, 4th Test

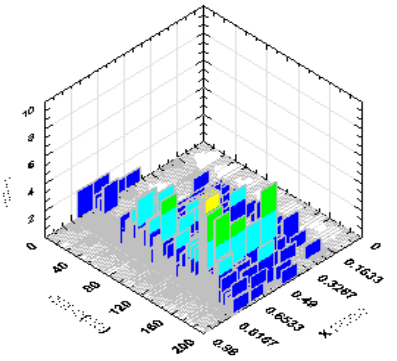

(c2) The Left Wing, 6th Test

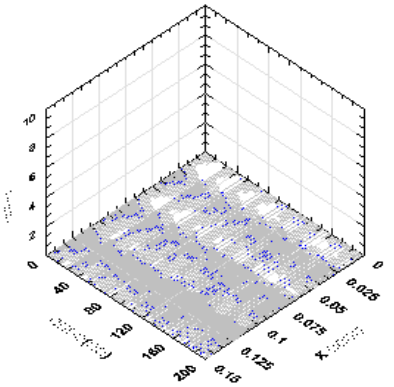

(d1) External Left Web, 4th Test

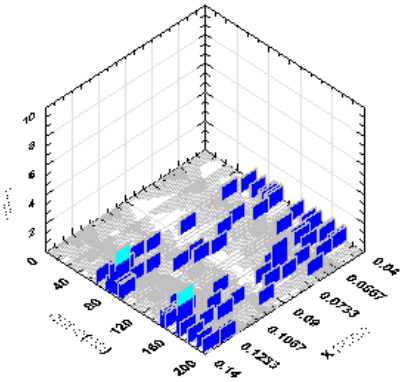

(d2) External Left Web, 6th Test

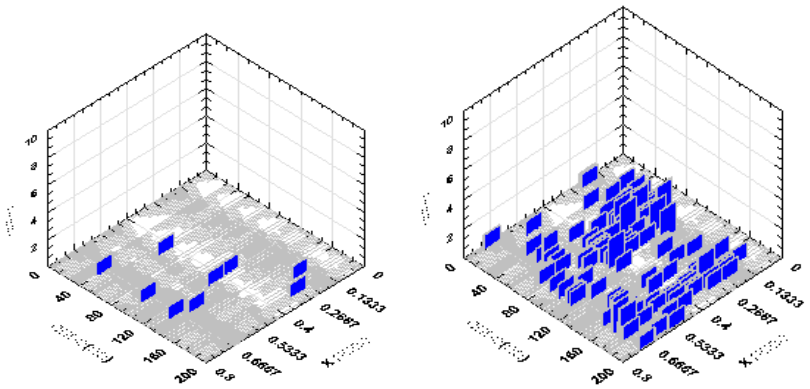

(e1) the right wing, 4th test (e2) the right wing, 6th test

Figure 14. Acoustic Emission Location Map under Condition 7

5. Analysis of Cracks and Structure Repair Plan

5.1 Analysis of Cracks

ANSYS simulation results show that Von Mises stresses do not exceed the allowable stress values during the whole process of boom luffing, both before and after the structure change. The thickness of the crack-occurred plate is 25 mm, the material is Q345, the yield strength is 325 MPa, and the allowable stress is 250Mpa according to relevant design code.

Nevertheless, it can be seen from Figure 7, the positions cracks occurred are in a complex stress state and stress concentration exists. In the crack location, X direction is mainly under tensile stress which gradually decreases along the Z and Y directions as the crack propagation direction. Along the Z direction within the length of the hinge support is always under tensile stress which gradually decreases and changes into compress stress along Y direction. Y direction is mainly under tensile stress, however, the tensile stress decreases rapidly along the X direction and the weld length is longer than that of Z direction, so that the crack did not extend in that direction; Z direction is mainly under compressive stress, but rapidly reduced tensile stress exists in the crack propagation direction.

The maximum stress of the Slew deck with pylon before the change is 190 MPa, and the location of it is the crack initiation position. The maximum stress after the change is 163 MPa, which is slightly less than before, and components of stress in X, Y, Z direction are reduced accordingly. Therefore the structure change is not the direct cause of crack.

We make a preliminary judgment that crack initiation locations lie in the multi-plate intersection region, whose welding process is complex and directly withstand large boom hinge point force and hinge point force of counterweight beam and oil cylinder passed through Slew deck with pylon, which leads to stress concentration and a complex three-way tensile stress state in the crack initiation position. The stress is large, which is approaching or has exceeded the fatigue limit stress, and bucket wheel stacker reclaimer dynamic loads pass directly through boom to crack initiation positions, which makes it easy to cause fatigue failure.

The internal and external inspections of cracks show that internal stiffeners on both sides of the Slew deck with pylon are asymmetrical, which may be the main reason of unlikeness of maximum stress and crack lengths on both sides. Acoustic emission test results show that the cracks and the bearing welds paralleled to them are active. Comparison of longitudinal data indicates a further increasing trend of cracks activity on both sides of the Slew deck with

pylon. Therefore, there is a urgent need for structural crack repair.

Before the repair, drivers of stacker reclaimers should pay attention to the following matters:

(1) Lower production efficiency, and stacker reclaimer workload should be appropriately reduced;

(2) Minimize the boom luffing and swivel motion in working condition with load, because with load, the boom luffing and swivel motion, particularly luffing motion, cause more damage to cracks of the Slew deck with pylon than in other working conditions;

(3) Strengthen the lubrication of transmission mechanisms and the structure hinge points to reduce frictional force and improve force condition in crack locations.

5.2 Structure Repair Plan

Structure repair plan is shown in Figure 15. After the repair, the max. Von Mises stress is 132 MPa in the crack region under boom luffing angle of 15 °. The stress distribution is shown in Figure 16.

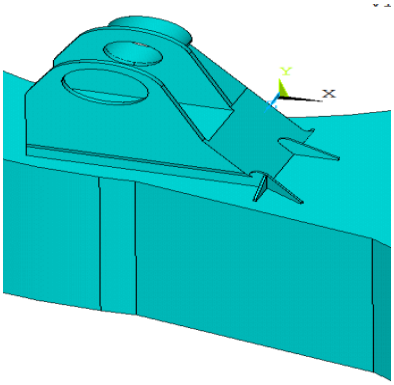

Figure 15. Structure Repair Plan

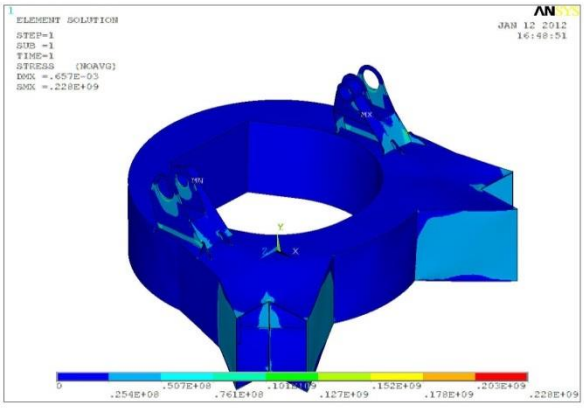

Figure 16. Von Mises Stress Distribution in Crack Locations After Repair

It can be seen that the max. stress is further reduced and the position of the max. stress changes after repair. Stresses in X, Y, Z direction are also reduced accordingly. Stresses at the cracks position vary from 25.4 MPa to 76.1 MPa, far less than the allowable stress, and stress concentration has been significantly reduced.

6. Conclusions

In this paper, using the finite element stress analysis and acoustic emission testing methods, the cracking problem of multi-plate interaction slew deck welded structure in bucket wheel stacker reclaimer for coal wharf was studied. Crack active status, crack propagation trend and cause reasons were comprehensively analyzed. On this basis, structure rectification measures and crack repair plan were proposed. The following conclusions can be drawn:

(1) In the crack initiation position, five plates interact with each other, where welding process is complex. And it is directly subjected to large reaction force of boom, counterweight beam and luffing oil cylinder hinge points as well as dynamic load from bucket wheel when stacking and reclaiming. This causes the multi-plate interaction region staying in three-way complex stress state and leads to stress concentration. The stress value is approaching to or may have exceeded the fatigue limit. That's the direct cause of the cracks, and the initial structural design is the essential problem. The maximum stress decreases after the structure change compared to before the change, which indicates bucket wheel changed to be chute is not the direct cause of the cracks.

(2) Adding 5.74 ton counterweight at the bucket wheel end can eliminate the unbalanced moment generated at the boom hinge point; combined with repair plan, the stress concentration at the cracks and stress at the Slew deck with pylon can be significantly reduced.

(3) Acoustic emission test results show that cracks on both sides of the Slew deck with pylon and the bearing welds paralleled to them are active and have a growing tendency, which is coincided with the predicted trend of finite element simulation. Acoustic emission testing can dynamically monitor trend and extent of crack propagation in real time. The method of using finite element simulation combined with acoustic emission testing provides an effective means to complex multi-plate intersection welded structure crack analysis and forecasting.

Acknowledgements

This work is sponsored by Shanghai Top Academic Discipline Project- Management Science & Engineering, this paper is supported by Doctoral Fund of the Ministry of Education（20123121120002, 20133121110001), Quality Standards and Metrology Research Project of the Ministry of Transport (2013-419-899-040) and Shanghai Education Committee Project "Shanghai Young College Teacher Training Subsidy Scheme", also supported in part by Ministry of Transport Research Projects (2012-329-810-180), Shanghai Municipal Education Commission Project (12ZZ148, 12ZZ149, 13YZ080).

References

[1] F. Wolfgang, "Review Fatigue analysis of welded joints: state of development", Marine Structures, vol.16, **(2003)**, pp. 185-200.
[2] T. R. Gurney and S. J.Maddox, "A re-analysis of fatigue data for welded joints in steel" Welding Research Int, vol. 3, no. 4, **(1973)**, pp. 1–54.
[3] R. Olivier and D. Ritter, "Catalogue of S–N curves of welded joints in structural steel", Dusseldorf: DVS-Verlag, vol. 1-5, no. 56, **(1979)**.
[4] S. V. Petinov, H. S. Reemsnyder and A. K. Thayamballi, "The similitude of fatigue damage principle: application in S–N curves-based fatigue design", Marquis G., Solin S., editors. Fatigue design and reliability. Amsterdam: Elsevier, **(1999)**.
[5] E. Niemi and P. Tanskanen, "Hot spot stress determination for welded edge gussets", Weld World, vol. 44, no. 5, **(2000)**, pp. 31–7.
[6] J. Y. Yung and F. V. Lawrence, "Analytical and graphical aids for the fatigue design of weldments", Fatigue

Fract Eng Mater Struct., vol.8, no. 3, , **(1985)**, pp. 223–41.
[7] R. J. Anthes, V. B. Kottgen and T. Seeger, "Notch factors of butt welds and cruciform joints (in German)", Schweien Schneiden, vol. 45, no. 12, **(1993)**, pp. 685–8.
[8] K. Iida and T. Uemura, "Stress concentration factors formulae widely used in Japan", Fatigue Fract Eng Mater Struct, vol. 19, no. 6, **(1996)**, pp. 779–86.
[9] H. P. Lehrke, "Calculation of stress concentration factors for welded joints (in German)", Konstruktion, vol. 51, no. 1/2, **(1999)**, pp. 47–52.
[10] F. V. Lawrence, R. Mattos and J. D. Burk, "Estimating the fatigue crack initiation life in welds", ASTM STP648 Philadelphia, **(1978)**, pp. 134-58.
[11] I. F. Smith and T. R. Gurney, "Changes in the fatigue life of plates with attachments due to geometrical effects", Welding J Res Suppl, vol. 65, no. (244s–50s), **(1986)**.
[12] S. T. Lie and S. Lan, "A boundary element analysis of misaligned load-carrying cruciform welded joints", Int J Fatigue, vol. 20, no. 6, **(1998)**, pp. 433–439.
[13] R. C. McClung, "Finite element analysis of fatigue crack closure: a historical and critical review", Wu XR, Wang ZG, editors. Proceedings of the Fatigue 99, Vol. I. Beijing: Higher Education Press, China.
[14] J. C. Newman Jr., E. P. Phillips and M. H. Swain, "Fatigue life prediction methodology using small crack theory", Int J Fatigue, vol. 21, no. (109–19), **(1999)**.
[15] C. Y. Hou and J. J. Charng, "Models for the estimation of weldment fatigue crack initiation life", Int. J Fatigue, vol. 19, no. 7, **(1997)**, pp. 537-541.

Author

Lu Kai-liang, received his PhD from Tongji University, Shanghai, China. Currently, he is working in Logistics Engineering College, Shanghai Maritime University (SMU) as an Associate Professor. His research interests include port machine structure and system dynamics, theory and method of dynamic design and optimization of structure, etc. He has 20 publications to his credit both in international and national Journals. He is a committee member of Shanghai Society of Theoretical & Applied Mechanics, member of China Construction Machinery Society (CCMS), and Logistics Engineering Institution, CMES.

